Non-Contact Measurement of Cardiac Electromagnetic Field in Mice by Use of a Microfabricated Atomic Magnetometer

B Lindseth[1,3], P Schwindt[2,3], J Kitching[3], D Fischer[4], V Shusterman[4,5]

[1]National Center for Atmospheric Research, Boulder, CO, USA
[2]Sandia National Laboratories, Albuquerque, NM, USA
[3]National Institute of Standards and Technology, Boulder, CO, USA
[4]University of Pittsburgh, Pittsburgh, PA, USA
[5]PinMed, Inc, Pittsburgh, PA, USA

Abstract

The development of clinical applications of magnetocardiography has been impeded by the large size of the systems used to measure magnetic fields. Here we present the first measurements of the cardiac electromagnetic field with a highly miniaturized (20 mm^3), atomic magnetometer constructed by microfabrication techniques. Measurements were performed in two mice. The magnetometer was placed close to the sternum region, approximately 2 mm away from the surface of the skin. QRS complexes were identifiable in the magnetocardiographic signals in all recordings except for those performed when the animal was moved far away (>10 cm) from the sensor. Non-contact recording of cardiac electromagnetic fields with a microfabricated magnetometer is feasible in a shielded environment.

1. Introduction

A number of studies have shown that magnetocardiography (MCG), particularly multichannel recordings, can provide useful information complementing electrocardiographic examination [1-3]. Previous studies in magnetocardiography include analysis of cardiac depolarization and repolarization patterns in MCG obtained from patients with cardiac arrhythmias and myocardial ischemia, as well as fetal and neonatal MCG [1]. More recently, methods for beat-to-beat MCG recording and analysis have been introduced, making MCG more attractive for clinical and experimental applications [4].

The devices of choice in previous studies of MCG applications were SQUID magnetometers, because their high sensitivity in measuring small magnetic fields allows one to obtain a high accuracy and spatial resolution in the measurement of cardiac magnetic fields [1-4]. The liquid-helium cooled, low-Tc SQUID intrinsic noise floor or magnetic field resolution, δB_{min}, is typically in the range between 1 and 10 fT Hz$^{-1/2}$, allowing reliable detection of the cardiac magnetic field signals, which are usually in the range of 50 to 100 pT [1]. A major drawback of SQUID magnetometry is the large size and cost of this cryogenically cooled equipment, which has made it unpractical for most medical institutions and research centers to obtain.

Thus, despite its long history and a number of advantages, the development of clinical applications of MCG has been impeded, at least in part, by the large size and cost of the magnetic-field measurement systems [1]. Here we present the first measurements of the cardiac electromagnetic field with a highly miniaturized (2 mm) atomic magnetometer constructed by microfabrication techniques.

Atomic magnetometers are based on the Larmor precession of atoms with nonzero angular momentum in a magnetic field, B_0 [5, 6]. The precession frequency is given by the Breit-Rabi formula, which can be approximated at low magnetic fields as $f_L = \gamma B_0$, where γ is the gyromagnetic constant of the atomic species being observed (28 kHz/μT for a free electron). By measuring this precession frequency, the magnetic field can be determined to high precision.

Several methods of measuring the Larmor precession frequency have been implemented, dating back to the 1960s. In one frequently used implementation [7], the atomic species are alkali atoms (^{39}K, ^{87}Rb or ^{133}Cs, for example) confined in a sealed cell with a buffer gas such as Ne. Alkali atoms have a single valence electron; the spin of this electron can be polarized by interaction with an appropriately polarized optical "pump" field in a process known as optical pumping. Once polarized, the atomic spins are excited to precess about the local static

magnetic field through the application of a transverse magnetic field, ΔB, oscillating at the Larmor precession frequency. The transverse field can be generated by a pair of coils driven by an AC generator. The magnitude and phase of the Larmor precession is read out with a second "probe" optical field. The operation of this type of magnetometer is shown schematically in Figure 1(a).

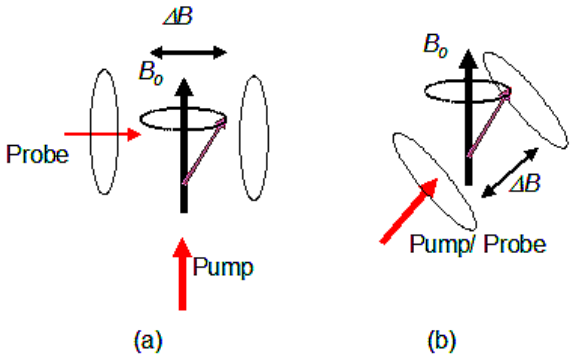

Figure 1 Magnetometers based on Larmor precession of alkali atoms. (a) Two-beam configuration with equatorial dead zone, (b) One-beam configuration with polar and equatorial dead zones.

The same optical field can in fact be used as both the polarizing mechanism and the readout, as shown in Figure 1(b). In this case, the static magnetic field to be measured must have components both parallel to the propagation direction of the light, to enable pumping, and perpendicular to the direction of the light, to enable a measurement of the transverse polarization component. Hence, such a magnetometer has "dead zones", field directions for which the sensor responsivity is zero, in directions both completely parallel and completely perpendicular to the light propagation direction. With the static field oriented at 45°, the responsivity is maximal.

Recent advances in atomic magnetometry have demonstrated exceptional sensitivity, comparable to [8-11], and even exceeding [12] the sensitivity of SQUID-based sensors. Table-top versions of these sensors have been demonstrated in applications including magnetic resonance imaging (MRI) [13], magnetic particle detection [14], MCG [15] and magnetoencephalography [12]. While these demonstrations show feasibility, further engineering and refinement of the apparatus is needed before such sensors could be widely used in health care or in the field.

2. Methods

2.1. Chip-scale atomic magnetometer

Highly miniaturized magnetometers based on fabrication techniques common in microelectro-mechanical systems (MEMS) promise to enhance the utility of atomic magnetometry in real-world applications. The field of MEMS deals with the fabrication of submillimeter mechanical structures by use of lithographic patterning and chemical etching. Processes have been developed that use MEMS to enable the fabrication of alkali vapor cells with dimensions on the order of 1 mm [16, 17]. In addition to their small size, the MEMS-based design potentially allows the fabrication of a large number of cells simultaneously with the same process sequence, which could lead to substantially reduced cost for large device volumes. The structure of the vapor cells and photographs of a typical cell are shown in Figure 2.

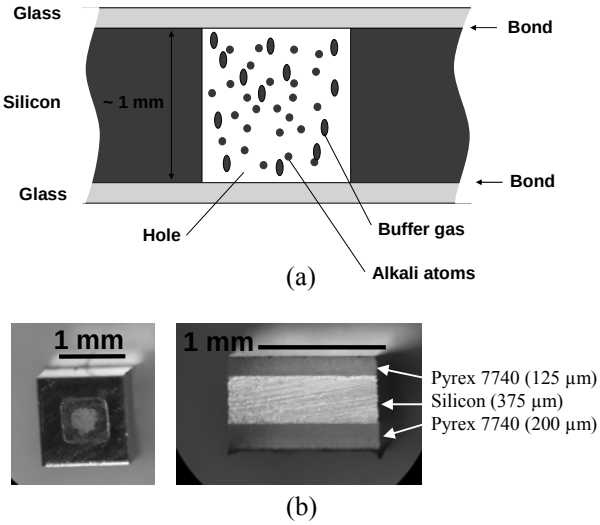

Figure 2. (a) Basic MEMS alkali vapor cell structure. A hole is etched in a Si wafer and glass wafers bonded to the upper and lower surfaces. Alkali atoms and a buffer gas are confined in the sealed volume. (b) Photographs of a MEMS vapor cell with a volume of 1 mm^3.

The vapor cells are integrated into a stacked structure, shown in Figure 3(a), that includes a semiconductor laser (1), a polymer spacer (2), optics to condition the emitted light field (3), low-magnetic-field heaters (4), the cell (5) and a photodetector to detect the transmitted optical power (6). The magnetometer has a total volume below 20 mm^3 and operates on about 200 mW of electrical power. When operated under ideal experimental conditions, the sensitivity of the instrument was $\delta B_{min} \sim 5$ pT/√Hz at frequencies between 1 Hz and 1 kHz. Details of the instrument can be found in Ref. [18].

An oscillating magnetic field was created near the Larmor precession frequency of the atoms by driving a

pair of microfabricated Helmholtz coils located on either side of the cell. The signal from the photodiode, caused by the Larmor precession of the atoms driven by the oscillating field, was demodulated with a lock-in amplifier to generate a dispersive "error signal" as a function of the static magnetic field. Because the direction of the heart magnetic field vector is typically oriented from head to tail of the animal, the animal was positioned at a 45 degree angle to the optical axis of the sensor, the most sensitive direction. A static magnetic field of 5.5 μT was applied parallel to this direction. The coil drive frequency was set to near the Larmor resonance at this field value, bringing the error signal close to zero. Small changes in the static magnetic field generated by the magnetic source therefore resulted in corresponding changes in the error signal.

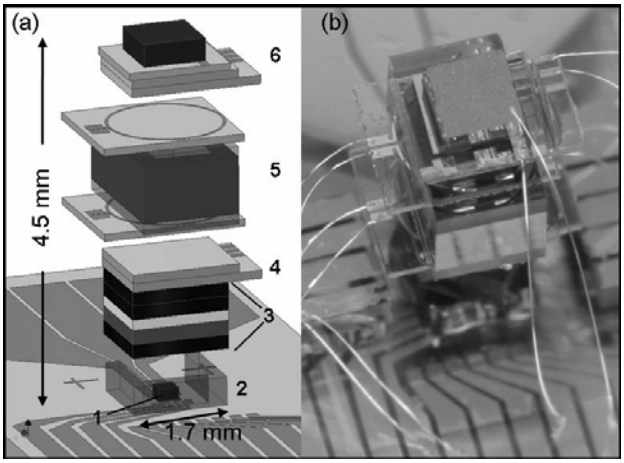

Figure 3. Structure and photograph of the NIST chip-scale atomic magnetometer (see Ref [18] for details).

2.2. Animal preparation and measurement procedure

Measurements were performed in two wild-type mice. Prior to the experiments, the animals were sedated and placed into a two-layer magnetic shield (Figure 4). Cardiac electrical potentials were measured by subcutaneous, nonmagnetic, copper electrodes in the standard, limb position. The magnetometer was placed close to the sternum region, approximately 2 mm away from the surface of the skin with the static field oriented roughly perpendicular to the skin surface. The electrocardiogram (ECG) and the magnetocardiogram (MCG) signals were fed into a multiplexer system and recorded simultaneously at 1 kHz per channel and 12-bit resolution for post-processing. To control for various mechanical artifacts, we performed the recordings, consecutively, as follows: (1) with the animal positioned above/below/far away from the sensor, and (2) with ECG electrodes connected/disconnected from the animal. *Signal processing*: R-peaks were detected in the ECG signals by a threshold-adaptive algorithm, and the ECG and MCG signals were averaged by use of the R-peaks as the fiducial points.

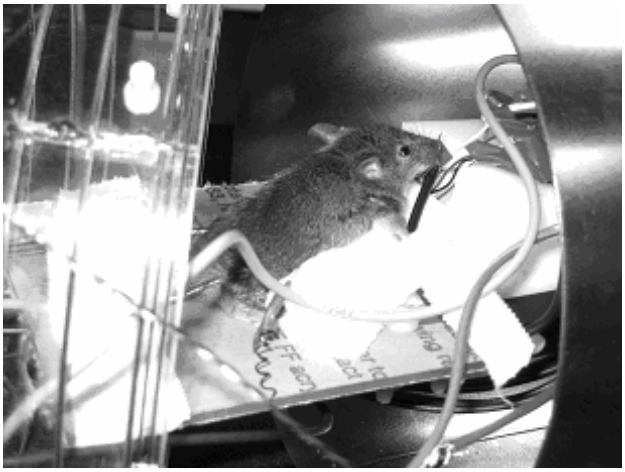

Figure 4. Experimental setup for magnetocardiographic recordings in a mouse, using a chip-scale atomic magnetometer. The magnetometer sensor is located approximately 2 mm below the skin of the animal in the sternum region, and it is covered by white plastic cover. A nonmagnetic electrocardiographic needle electrode and its wire are visible in front of the animal. The magnetic shield (on the left and right sides of the figure) is open for the pupose of taking the photograph.

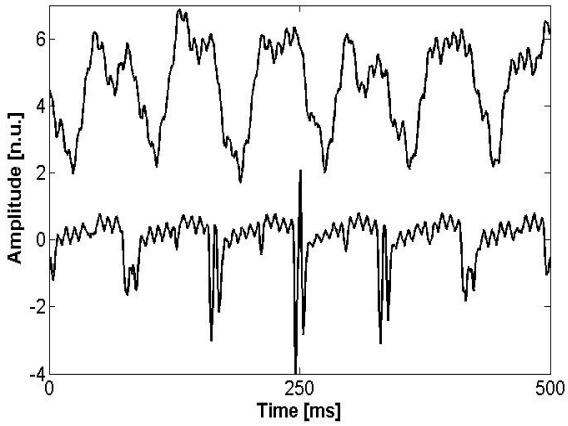

Figure 5. Signal-averaged magnetocardiographic (top) and electrocardiographic (bottom) signals recorded simultaneously and averaged over 50 cycles using R-peaks of the electrocardiogram as fiducial points. Signal amplitudes are in normalized units (n.u.). See text for details.

3. Results

QRS complexes were identifiable in the magnetocardiographic signals in all recordings except for those performed when the animal was moved far away from the sensor (> 10 cm). The QRS complexes became identifiable with the averaging of > 20 cardiac cycles (Figure 5). There was a time lag (~ 10 ms) between the QRS in the ECG and MCG signals and some loss of the high-frequency components in the MCG signal due to the suboptimal sampling of the real-time MCG filter.

4. Conclusions

Non-contact recording of cardiac electromagnetic fields with a microfabricated magnetometer is feasible in a shielded environment. Further refinements in signal processing should improve the quality of MCG recordings and might allow recordings in unshielded environment.

Acknowledgements

This study was supported in part by NIH grant HL077116 (VS). This work is a partial contribution of NIST and is not subject to copyright. The authors thank S. Knappe for fabricating the alkali vapor cell and useful discussions.

References

[1] Sternickel K, Braginski A. Biomagnetism using SQUIDs: status and perspectives. Superconducting Science and Technology 2006;19:S160-S171.

[2] Takala P, et al., Comparison of magnetocardiographic and electrocardiographic exercise mapping in healthy volunteers, presented at Recent Advances in Biomagnetism: Proc. 11th Int. Conf. on Biomagnetism, 1999.

[3] Van Leeuwen P, Hailer B, Lange S, Donker D, Grönemeyer D. Spatial and temporal changes during the QT-interval in the magnetic field of patients with coronary artery disease. Biomedical Technology 1999;44:139-142.

[4] Takala P, et al. Beat-to-beat analysis method for magnetocardiographic recordings during interventions. Phys. Med. Biol 2001;46:975-982.

[5] Bell WE, Bloom A. Optical detection of magnetic resonance in alkali metal vapor, Physical Review 1957; 107:1559-1565.

[6] Dehmelt HG. Slow spin relaxation of optically polarized sodium atoms. Physical Review 1957;105:1487-1489.

[7] Bloom A. Principles of operation of the Rubidium vapor magnetometer. Applied Optics 1962;1:61-68.

[8] Alexandrov EB, Balabas MV, Pasgalev AS, Vershovskii AK, Yakobson NN, Double-resonance atomic magnetometers: From gas discharge to laser pumping. Laser Physics 1996;6:244-251.

[9] Budker D, Kimball DF, Rochester SM, Yashchuk VV, Zolotorev M, Sensitive magnetometry based on nonlinear magneto-optical rotation. Physical Review A 2000;6204: 043403.

[10] Kominis IK, Kornack TW, Allred JC, Romalis MV. A subfemtotesla multichannel atomic magnetometer. Nature 2003;422:596-599.

[11] Groeger S, Bison G, Schenker JL, Wynands R, Weis A. A high-sensitivity laser-pumped M-x magnetometer. European Physical Journal D 2006;38:239-247.

[12] Xia H, Baranga ABA, Hoffman D, Romalis MV, Magnetoencephalography with an atomic magnetometer. Applied Physics Letters 2006;89:211104.

[13] Xu SJ, et al., Magnetic resonance imaging with an optical atomic magnetometer. Proceedings of the National Academy of Sciences of the United States of America, 2006;103:12668-12671.

[14] Xu SJ, et al., Application of atomic magnetometry in magnetic particle detection. Applied Physics Letters 2006; 89:224105.

[15] Bison G, Wynands R, Weis A. Dynamical mapping of the human cardiomagnetic field with a room-temperature, laser-optical sensor. Optics Express 2003;11:904-909.

[16] Liew LA, et al. Microfabricated alkali atom vapor cells. Applied Physics Letters 2004;84:2694-2696.

[17] Knappe S, et al., Atomic vapor cells for chip-scale atomic clocks with improved long-term frequency stability. Optics Letters 2005;30:2351-2353.

[18] Schwindt PDD, et al. A chip-scale atomic magnetometer with improved sensitivity using the Mx technique. Applied Physics Letters, 2007; 90:081102.

Address for correspondence:

Vladimir Shusterman
200 Lothrop Street, Room B535,
Pittsburgh, PA 15213
shustermanv@upmc.edu